The expansion/contraction of gold microparticles during voltammetrically induced amalgamation leads to mechanical instability†

Laura E. Barrosse-Antle,[a] Lei Xiao,[a] Gregory G. Wildgoose,[a] Ronan Baron,[a] Chris J. Salter,[b] Alison Crossley[b] and Richard G. Compton*[a]

Received (in Durham, UK) 8th May 2007, Accepted 13th July 2007
First published as an Advance Article on the web 7th August 2007
DOI: 10.1039/b706810g

The mechanical stability of gold microparticles during anodic stripping voltammetric (ASV) detection over a large range of mercury concentrations was investigated. Mercury was detected at gold microparticles chemically deposited onto glassy carbon microspheres using ASV. Oxidation was observed at 0.5 and 0.8 V *vs.* SCE. Which peak was observed was dependent on the concentration of mercury and the deposition potential. The formation of the amalgam was of interest. As mercury was deposited for longer time intervals, scanning electron microscopy (SEM) analysis showed the microparticles increasing in size from 0.76 ± 0.03 μm (initial) to 1.51 ± 0.14 μm (Hg^{2+} deposited for 1980 s at 0.35 V) in diameter. In order to ascertain if multiple expansion and contraction cycles damaged the gold microparticles, cyclic voltammetry was used to monitor the amount of gold on the electrode as mercury was deposited and stripped repeatedly. It was seen that the area under the cathodic gold peak decreased with repetitive scans. SEM analysis revealed that the mechanical stress of repetitive deposition and stripping cycles of mercury caused the gold microparticles to fracture, appearing as irregular cuboid crystals rather than as the orderly polycrystallite formations seen initially. Energy dispersive X-ray (EDX) analysis indicated that the composition of the microparticles changed over the course of repetitive deposition and stripping cycles from gold to an Au–Hg amalgam, which may not be in electrical contact with the carbon support.

1. Introduction

Mercury is a toxic compound, which nevertheless is extensively employed over a range of applications. Organomercury compounds are used in fungicides, antiseptics, preservatives and pharmaceuticals. Elemental mercury is itself a crucial component in certain types of instrumentation and industrial processes.[1] Inorganic mercury released into the environment by both natural and man-made processes—primarily volcanic activity and coal combustion—is able to enter the food chain *via* the action of methylating bacteria. Most mercury poisoning that is not related to occupational hazards results from the consumption of carnivorous fish in which organomercury compounds, in particular methyl mercury, have been concentrated due to biomagnification.[1]

Inorganic mercury primarily affects the kidneys, while organic mercury attacks the nervous system, causing tremors, muscle weakness, and impaired mental capacity, among other symptoms.[1] Toxic doses of either form result in shock, cardiovascular collapse, renal failure, and gastrointestinal damage.[1] Thus, accurate and sensitive quantitative analysis is essential to monitor the mercury content in foodstuffs and groundwater.

Currently, the World Health Organization recommends the use of flame atomic absorption spectroscopy (AAS) or cold vapour AAS for the determination of mercury.[1] The wealth of literature on the spectrochemical methods used for mercury detection testifies to the methods' utility.[2–6] However, spectroscopic techniques are far from ideal for use in "field" conditions. Electrochemical detection has come to the fore as a means of providing a cheap, rapid, facile, and portable method of mercury detection in the field. Methods exploiting these strengths have been and are in the process of being developed. Frequently these methods employ anodic stripping voltammetric techniques (ASV) involving a preconcentration or deposition step before detection, particularly for trace analysis.[7]

Although many types of electrode substrates have been investigated, gold electrodes are of particular interest due to the high affinity of gold towards mercury and thus have been extensively employed.[8–11] The same affinity that enhances the preconcentration of mercury at the electrode surface, however, can also be a severe disadvantage. Under high mercury concentrations, preconcentration can cause the mercury to diffuse far enough into the gold electrode that it cannot be completely stripped away.[12] Watson *et al.* suggest that bulk deposition of mercury irreversibly changes the nature of the electrode, forming a gold–mercury alloy electrode. Even repeated

[a] *Physical and Theoretical Chemistry Laboratory, University of Oxford, South Parks Road, Oxford, UK OX1 3QZ. E-mail: richard.compton@chemistry.oxford.ac.uk; Fax: +44 (0) 1865 275 410; Tel: +44 (0) 1865 275 413*
[b] *Department of Materials, University of Oxford, Parks Road, Oxford, UK OX1 3PH*

† Electronic supplementary information (ESI) available: EDX spectrum of gold microparticles on glassy carbon microspheres. See DOI: 10.1039/b706810g

stripping and cleaning is insufficient to restore the electrode to its original condition.[13]

Therefore studies into the detection of mercury at gold electrodes have begun to focus on renewable gold electrodes such as gold films.[10,11,14,15] These surfaces can be stripped away as they become amalgamated and subsequently regenerated, avoiding any deleterious change in their electrochemical properties. Gold microarrays, for which the fouling of a few individual elements does not significantly impair the overall electrode function, have also been investigated.[16] The use of gold particles has only just begun to be fully explored with regard to electrochemical mercury detection; Welch *et al.* have described some of the characteristics and potential applications of amalgamated gold nanoparticles,[17] whilst Keebaugh *et al.* have used the change in the resistance of gold nanowires to monitor the concentration of mercury in both the vapour and solution phase.[18] Another group has used self-assembling gold nanoparticles as a substrate for urease, the inhibition of which by mercury(II) is sensed potentiometrically.[19]

The present work is concerned with understanding the processes occurring during the detection of mercury at gold microparticles that are chemically deposited onto glassy carbon microspheres (Au-μp-GCs). Specifically, the mechanical stability of the gold microparticles during the ASV detection of a large range of mercury concentrations is investigated. Repetitive expansion during deposition and contraction during stripping is shown to be deleterious to the mechanical stability of the gold microparticles, causing the microparticles to fracture and become irregular in morphology as well as changing the composition of the microparticles from bulk gold to Au–Hg amalgam. An understanding of the amalgamation and stripping processes at gold microparticle modified electrodes may proffer opportunities for enhanced mercury detection using these materials.

2. Experimental

2.1 Reagents and instrumentation

Glassy carbon microspheres (10–20 μm) and gold sodium thiosulfate ($AuNa(S_2O_3)_2 \cdot H_2O$, 99.9%) were purchased from Alfa Aesar (Heysham, UK). L-ascorbic acid ($C_6H_8O_6$, 99%), mercury(II) nitrate monohydrate ($Hg(NO_3)_2$, 98%), nitric acid (HNO_3, 70%) and sodium hydroxide (97%) were purchased from Aldrich (Gillingham, UK). Dimethylformamide (reagent grade) was purchased from Fisher (Loughborough, UK). Aqueous solutions were prepared using deionised water (Vivendi, High Wycombe, UK) of resistivity not less than 18.2 MΩ cm at 25 °C.

Cyclic voltammetry and linear sweep voltammetry were performed using a type II μAutolab (Eco Chemie, Utrecht, Netherlands) which was interfaced with a PC using GPES (version 4.9) software for Windows. Measurements were performed using a three-electrode cell of 10 mL. The working electrode consisted of Au-μp-GCs abrasively immobilised onto a basal-plane pyrolytic graphite (bppg) electrode. A platinum wire was used as the counter electrode, and a silver wire or a saturated calomel electrode (SCE) (Radiometer, Copenhagen, Denmark) was used as the quasi-reference or reference electrode, respectively. All potentials measured *vs.* silver wire were calibrated against the SCE and are reported *vs.* SCE. A scan rate of 50 mV s^{-1} was used unless otherwise stated. All electrochemical measurements were performed in 0.1 M HNO_3.

SEM was carried out using a JEOL 6500F instrument. The compositional analysis of the gold microparticles on the electrode surface was done by employing wavelength dispersive X-ray spectrometry (WDS; Jeol JXA-8800 microprobe).[20]

2.2 Microparticle fabrication

The gold microparticles were formed on the glassy carbon microspheres *via* electroless reduction of gold sodium thiosulfate using L-ascorbic acid as the reducing agent. Glassy carbon microspheres (200 mg) were dispersed in 100 mL of pure water and sonicated for one minute. The suspension was then stirred during the addition of gold sodium thiosulfate (150 mg). The flask was covered in foil, and L-ascorbic acid (90 mg) was added slowly. The solution was stirred for 18 hours before being vacuum filtered and washed with deionised water. The resulting Au-μp-GC powder was dried at 100 °C for 2 hours prior to use.

2.3 Immobilisation of Au-μp-GCs on bppg electrode

The Au-μp-GC powder was abrasively immobilised onto the surface of a bppg electrode.[21] This was done by polishing the electrode on silicon carbide paper (P1000) and then removing the upper layers of graphite using adhesive tape. The Au-μp-GCs were then immobilised onto the bppg electrode by gently rubbing the electrode surface on a fine qualitative filter paper (Whatman) containing the Au-μp-GC powder.

3. Results and discussion

3.1 Characterisation of Au-μp-GCs

The presence of gold on the glassy carbon microspheres was confirmed by cyclic voltammetry. The Au-μp-GC powder was abrasively immobilised onto a basal-plane pyrolytic graphite (bppg) electrode and scanned from 0 to 1.4 V *vs.* SCE. Oxidation of bulk gold was observed as an anodic peak at 1.2 V that was partially obscured by the effect of solvent breakdown. The corresponding reduction peak was clearly resolved at 0.8 V. The gold fingerprint of the abrasively modified bppg is overlaid on a cyclic voltammogram of the unmodified bppg in Fig. 1. Scanning electron microscopy (SEM) was used to confirm that the chemical deposition of gold microparticles onto glassy carbon microspheres had been successful, with gold microparticles with an average diameter of 0.76 ± 0.03 μm ($n = 82$) clearly evident on the surface of the glassy carbon microspheres (Fig. 2).

3.2 Voltammetry of mercury detected at Au-μp-GCs

Initially the linear sweep anodic stripping voltammetry (LSASV) detection of mercury(II) nitrate was performed over a wide potential window, from 0.15 to 1.05 V *vs.* SCE, after deposition at 0.15 V for 30 s. Two sharp, well-defined peaks were observed at 0.43 and 0.50 V and a third broad peak at

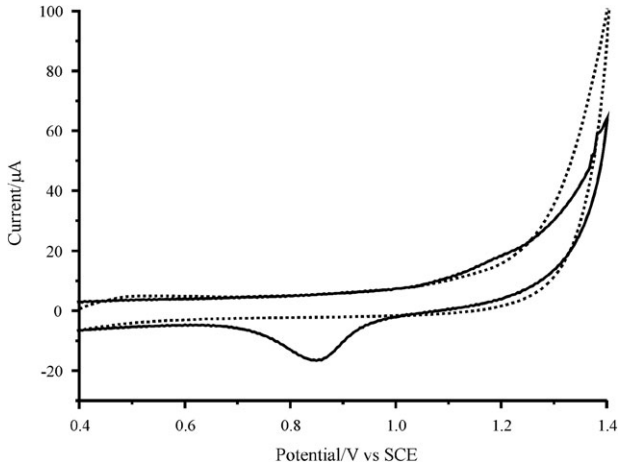

Fig. 1 Cyclic voltammetry confirming the presence of gold microparticles on glassy carbon microspheres (Au-μp-GCs) abrasively immobilised on a basal-plane pyrolytic graphite electrode (bppg). Scan performed in 0.1 M HNO_3 at 50 mV s^{-1}. The dashed line shows the response of an unmodified bppg, and the solid line shows the response of a bppg with gold present.

0.85 V. Comparative scans using glassy carbon (GC), unmodified bppg, and bulk gold electrodes revealed that, at the high concentration of 120 μM Hg^{2+}, the peak occurring at 0.85 V can be attributed to mercury stripping from gold. The oxidative stripping at lower potentials can be attributed to the stripping of mercury deposited on the carbon components (GC and bppg) of the abrasively modified electrode. To selectively deposit mercury solely on the gold microparticles, the deposition potential was altered to +0.35 V, with the subsequent scans performed over the potential range 0.35–1.1 V.

According to Schadewald *et al.*, deposition of mercury onto the surface of a gold electrode in excess of a monolayer results in diffusion of the mercury into the gold surface. This creates a Au–Hg alloy, which is subsequently stripped at approximately 0.8 V *vs.* SCE. Bulk mercury that has not diffused into the electrode is then stripped from the surface at 0.4 V.[12] At the high concentrations initially examined, only alloy stripping was observed, as seen in Fig. 3. When the mercury concentration was reduced and the parameters were adjusted to deposit at and scan from 0.2 V, a small peak attributed to bulk stripping of mercury from gold was observed at 0.48 V. This peak, seen in Fig. 4, appeared at the base of the carbon peaks, which reappeared at the less positive deposition potential.

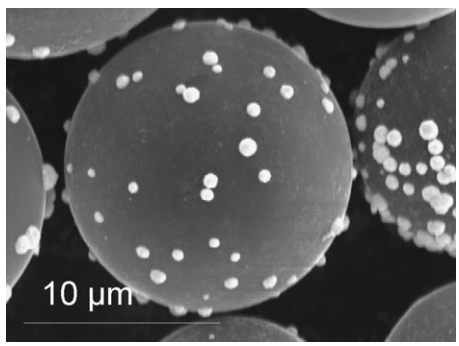

Fig. 2 Scanning electron microscope (SEM) image of glassy carbon microspheres after chemical deposition of gold microparticles.

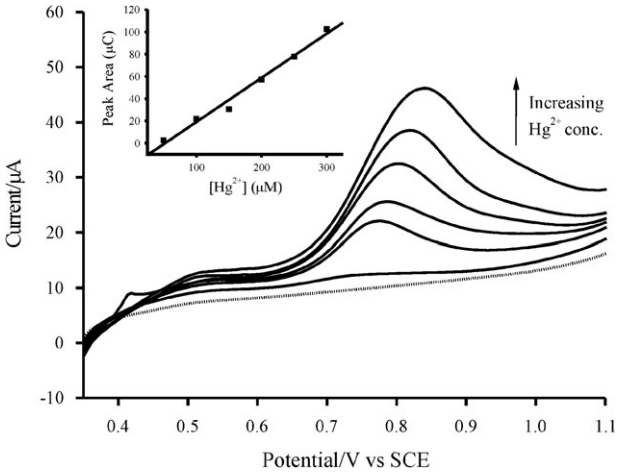

Fig. 3 Linear sweep voltammetry (LSV) of 50 μM additions of mercury(II) nitrate to a 0.1 M HNO_3 solution at 50 mV s^{-1}. Mercury was deposited for 60 s at 0.35 V. The inset shows linear response to mercury over the concentration range of 0–300 μM.

3.3 Mechanical instability of Au-μp-GCs

The amalgamation process was of particular interest to the authors. The literature concerning underpotential deposition and stripping (UPD and UPS, respectively) of mercury on gold is largely concerned with bulk gold electrodes. Thus the stripping of mercury from any Au–Hg alloy formed does not result in significant structural change to the bulk electrode, though an increase in surface roughness has been observed.[12] To better understand the ramifications of UPS with regard to gold microparticles, a series of depositions were performed. Mercury(II) (100 μM) was deposited at 0.35 V for 60 s and scanned from 0.35 to 1.1 V. Then the electrode was removed from the Hg^{2+} solution and placed into 0.1 M HNO_3. A cyclic

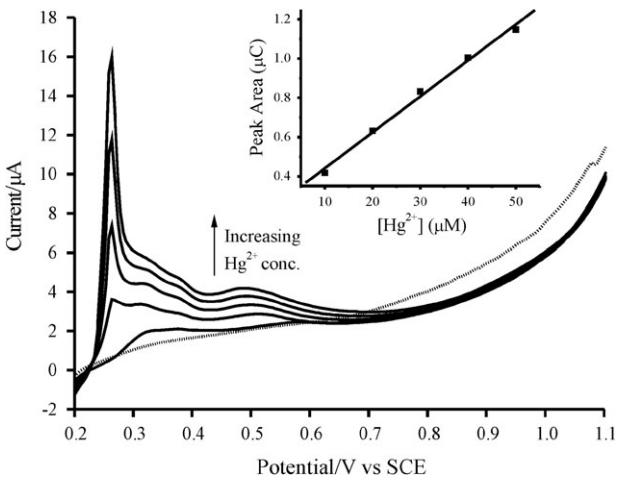

Fig. 4 LSV of 10 μM additions of mercury(II) nitrate to a 0.1 M HNO_3 solution at 50 mV s^{-1}. Mercury was deposited for 30 s at 0.2 V. Peaks at 0.25, 0.32, and 0.38 V show carbon response to mercury. The peak at 0.48 V is the gold response to mercury. The inset shows linear response to mercury over the concentration range of 0–50 μM.

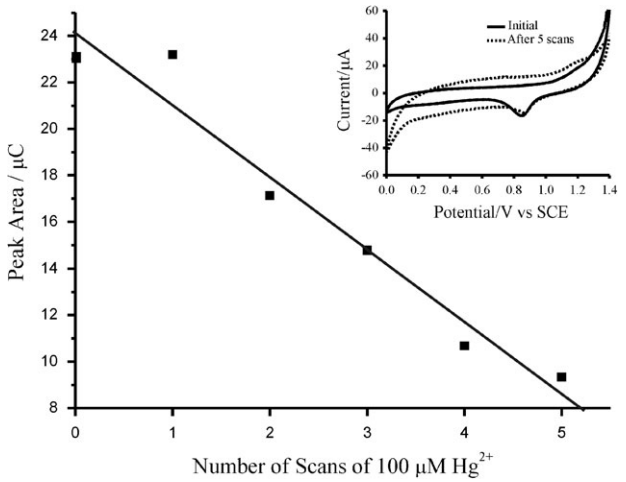

Fig. 5 Decrease in peak area associated with gold reduction is correlated with the number of deposition and stripping steps of 100 μM mercury(II) nitrate on a bppg modified with Au-μp-GCs. The inset shows cyclic voltammetry taken before and after five deposition and stripping steps were performed.

voltammogram over the gold fingerprint range (0–1.4 V) was taken and the area under the cathodic peak measured. A plot of peak areas obtained in this fashion shows a linear decrease in the amount of electroactive gold at the electrode with repetitive scans (Fig. 5). One possible reason for the decrease is a gradual detachment of the Au-μp-GCs from the electrode surface. However, when the same procedure was performed in the absence of mercury, the decrease in gold was less than that observed when mercury is stripped from it, and therefore the decrease in electroactive gold cannot be explained by the Au-μp-GCs simply falling off in solution. Thus it was posited that repetitive stripping of the Au–Hg amalgam damaged the microparticles, causing some gold to be stripped away with the mercury and resulting in a decrease in both the amount of gold present on the electrode and the resulting electroanalytical performance.

In order to better understand the processes involved, three samples of microparticles were imaged using SEM. Fig. 6a shows microparticles after being partially saturated (400 μM Hg^{2+} deposited for 990 s at 0.35 V). They are larger than the original sample shown in Fig. 2, with an average diameter of 0.96 ± 0.04 μm (n = 76). The volume of the spheres is doubled, though no major morphological changes are observed. When the microparticles are saturated (400 μM Hg^{2+} deposited for 1980 s at 0.35 V), their size is found to increase dramatically, enlarging to approximately nine times their original volume. Their average diameter is 1.51 ± 0.14 μm (n = 91), as shown in Fig. 6b, and the microparticles appear flattened. In some cases, the microparticles expand into each other to the point that they are barely distinguishable as discrete units. In that situation, they appear to pull away from close contact with the surface of the glassy carbon microspheres, possibly leading to detachment of the Au–Hg alloy.

Fig. 7b shows a high resolution image of microparticles that have undergone repetitive deposition and stripping cycles. Mercury(II) (400 μM) was deposited at 0.35 V for 990 s and then scanned from 0.35 to 1.1 V. This process was repeated

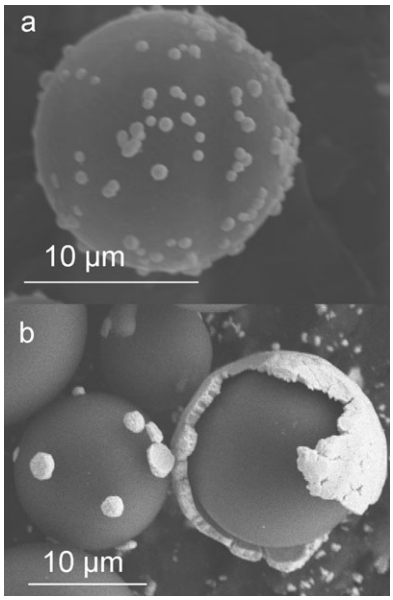

Fig. 6 SEM images of gold microparticles on glassy carbon microspheres after deposition of 400 μM mercury(II) nitrate at 0.35 V for (a) 990 s and (b) 1980 s.

seven times. There is an obvious change in morphology from the original particle to the repetitively stripped particle. Energy dispersive X-ray (EDX) analysis showed that the microparticles are composed of gold, mercury (the ratio varying) and a trace amount of chloride. These repetitively expanded and contracted amalgam microparticles were larger than both the original and half-saturated microparticles, with an average diameter of 1.14 ± 0.08 μm (n = 34). Comparison of the morphology of damaged amalgam microparticles with that of the original microparticles as seen using high definition SEM (Fig. 7a) reveals distinct differences. Most notably, the original cabbage-like arrangement of gold polycrystallites is no longer

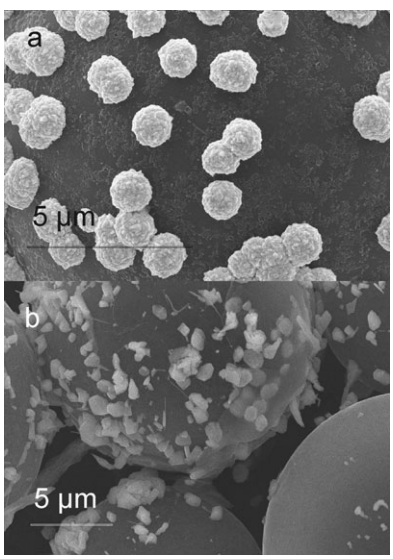

Fig. 7 High resolution SEM images of (a) gold microparticles prior to exposure to mercury and (b) Au–Hg microparticles after seven successive deposition and scanning steps in 400 μM mercury(II) nitrate (mercury deposited for 990 s at 0.35 V).

observed. Instead, the microparticles appear cuboid and irregular. They appear to be individual crystals and are not symmetrically grouped. It is clear that the morphology of the gold microparticles has changed during the repetitive electrochemical deposition and stripping of mercury.

These observations, taken in context with the cyclic voltammetry showing the decreasing amount of gold on the surface, suggest that the stripping events oxidise some combination of mercury and gold, altering the composition of the remaining microparticles until a stable amalgam is left on the carbon surface. However, note that the amalgam may not be in electrical contact with carbon. The mechanical stress of this process fractures the ordered polycrystallites, resulting in the irregular morphology of the remaining microparticles.

Conclusion

The oxidation of mercury on gold microparticles chemically deposited on glassy carbon microspheres follows patterns observed in the literature. Anodic peaks at 0.5 V and 0.8 V were seen and attributed to the stripping of bulk mercury and the stripping of Au–Hg amalgam, respectively. Due to the size of the microparticles, the processes that cause pitting in bulk gold electrodes caused destruction of the original gold microparticles. SEM and EDX analyses, combined with voltammetry, show a decrease in the amount of gold on the surface, indicating that repetitive deposition and stripping of mercury from gold microparticles results in drastic morphological and compositional changes due to the mechanical stresses induced by the expansion and contraction cycles. The knowledge of the mechanical instability of gold microparticles with repetitive deposition and stripping cycles should guide their application in electrochemical sensing of mercury(II). Practicality dictates that easily renewable gold micro- and nanoparticle-based sensors continue to be explored in order to achieve the maximum reproducible range of mercury(II) detection on a gold surface.

Acknowledgements

L.E.B.-A. thanks the Physical and Theoretical Chemistry Laboratory for financial support. G.G.W. thanks St. John's College for a Junior Research Fellowship. L.X. thanks Windsor Scientific and the EPSRC for an Industrial CASE award.

References

1 J. K. Fawell, J. Cortruvo, M. Giddings, P. Jackson, Y. Magara and E. Ohanian, *Mercury in Drinking-Water: Background Document for Development of WHO Guidelines for Drinking-Water Quality*, World Health Organization, Geneva, Switzerland, 2005.
2 N. S. Bloom and E. A. Crecelius, *Mar. Chem.*, 1983, **14**, 49–59.
3 Å. Iverfeldt, *Water, Air, Soil Pollut.*, 1991, **56**, 251–265.
4 P. Porvari and M. Verta, *Environ. Pollut.*, 2003, **123**, 181–191.
5 J. Schäfer, G. Blanc, S. Audry, D. Cossa and C. Bossy, *Appl. Geochem.*, 2006, **21**, 515–527.
6 G. R. Wall, H. H. Ingleston and S. Litten, *Water, Air, Soil Pollut.*, 2005, **165**, 233–248.
7 *Method 7472: Mercury in Aqueous Samples and Extracts by Anodic Stripping Voltammetry (ASV)*, ed. United States Environmental Protection Agency, Washington, DC, 1996.
8 Y. Bonfil, M. Brand and E. Kirowa-Eisner, *Anal. Chim. Acta*, 2000, **424**, 65–76.
9 H. G. Jayaratna, *Curr. Sep.*, 1997, **16**, 93.
10 P. Richter, M. I. Toral and B. Abbott, *Electroanalysis*, 2002, **14**, 1288–1293.
11 E. A. Viltchinskaia, L. L. Zeigman and S. G. Morton, *Electroanalysis*, 1995, **7**, 264–269.
12 L. A. Schadewald, T. R. Lindstrom, W. Hussein, E. E. Evenson and D. C. Johnson, *J. Electrochem. Soc.*, 1984, **131**, 1583–1587.
13 C. M. Watson, D. J. Dwyer, J. C. Andle, A. E. Bruce and M. R. M. Bruce, *Anal. Chem.*, 1999, **71**, 3181–3186.
14 M. A. Augelli, R. A. A. Munoz, E. M. Richter, A. J. Gouveia and L. Angnes, *Electroanalysis*, 2005, **17**, 755–761.
15 N. Kariuki, L. B. Isreal, M. M. Maye and C.-J. Zhong, in *222nd ACS National Meeting*, American Chemical Society, Chicago, IL, USA, 2001.
16 O. Ordeig, C. E. Banks, J. del Campo, F. X. Muñoz and R. G. Compton, *Electroanalysis*, 2006, **18**, 573–578.
17 C. M. Welch, O. Nekrassova, X. Dai, M. E. Hyde and R. G. Compton, *ChemPhysChem*, 2004, **5**, 1405–1410.
18 S. Keebaugh, A. K. Kalkan, W. J. Nam and S. J. Fonash, *Electrochem. Solid-State Lett.*, 2006, **9**, H88–H91.
19 Y. Yang, Z. Wang, M. Yang, M. Guo, Z. Wu and G. Shen, *Sens. Actuators, B*, 2006, **114**, 1.
20 K. Jurkschat, S. J. Wilkins, C. J. Salter, H. C. Leventis, G. G. Wildgoose, L. Jiang, T. G. J. Jones, A. Crossley and R. G. Compton, *Small*, 2006, **2**, 95–98.
21 G. G. Wildgoose, M. Pandurangappa, N. S. Lawrence, L. Jiang, T. G. J. Jones and R. G. Compton, *Talanta*, 2003, **60**, 887–893.